$1p_{3/2}$ Proton-Hole State in ^{132}Sn and the Shell Structure Along $N = 82$

J. Taprogge,[1,2,3] A. Jungclaus,[1,*] H. Grawe,[4] S. Nishimura,[3] P. Doornenbal,[3] G. Lorusso,[3] G. S. Simpson,[5] P.-A. Söderström,[3] T. Sumikama,[6] Z. Y. Xu,[7] H. Baba,[3] F. Browne,[8,3] N. Fukuda,[3] R. Gernhäuser,[9] G. Gey,[5,10,3] N. Inabe,[3] T. Isobe,[3] H. S. Jung,[11,†] D. Kameda,[3] G. D. Kim,[12] Y.-K. Kim,[12,13] I. Kojouharov,[4] T. Kubo,[3] N. Kurz,[4] Y. K. Kwon,[12] Z. Li,[14] H. Sakurai,[3,7] H. Schaffner,[4] K. Steiger,[9] H. Suzuki,[3] H. Takeda,[3] Zs. Vajta,[15,3] H. Watanabe,[3] J. Wu,[14,3] A. Yagi,[16] K. Yoshinaga,[17] G. Benzoni,[18] S. Bönig,[19] K. Y. Chae,[20] L. Coraggio,[21] A. Covello,[21,22] J.-M. Daugas,[23] F. Drouet,[5] A. Gadea,[24] A. Gargano,[21] S. Ilieva,[19] F. G. Kondev,[25] T. Kröll,[19] G. J. Lane,[26] A. Montaner-Pizá,[24] K. Moschner,[27] D. Mücher,[9] F. Naqvi,[28] M. Niikura,[7] H. Nishibata,[16] A. Odahara,[16] R. Orlandi,[29,30] Z. Patel,[31] Zs. Podolyák,[31] and A. Wendt[27]

[1]*Instituto de Estructura de la Materia, CSIC, E-28006 Madrid, Spain*
[2]*Departamento de Física Teórica, Universidad Autónoma de Madrid, E-28049 Madrid, Spain*
[3]*RIKEN Nishina Center, RIKEN, 2-1 Hirosawa, Wako-shi, Saitama 351-0198, Japan*
[4]*GSI Helmholtzzentrum für Schwerionenforschung GmbH, 64291 Darmstadt, Germany*
[5]*LPSC, Université Joseph Fourier Grenoble 1, CNRS/IN2P3, Institut National Polytechnique de Grenoble, F-38026 Grenoble Cedex, France*
[6]*Department of Physics, Tohoku University, Aoba, Sendai, Miyagi 980-8578, Japan*
[7]*Department of Physics, University of Tokyo, Hongo 7-3-1, Bunkyo-ku, 113-0033 Tokyo, Japan*
[8]*School of Computing, Engineering and Mathematics, University of Brighton, Brighton BN2 4JG, United Kingdom*
[9]*Physik Department E12, Technische Universität München, D-85748 Garching, Germany*
[10]*Institut Laue-Langevin, B.P. 156, F-38042 Grenoble Cedex 9, France*
[11]*Department of Physics, Chung-Ang University, Seoul 156-756, Republic of Korea*
[12]*Rare Isotope Science Project, Institute for Basic Science, Daejeon 305-811, Republic of Korea*
[13]*Department of Nuclear Engineering, Hanyang University, Seoul 133-791, Republic of Korea*
[14]*School of Physics and State key Laboratory of Nuclear Physics and Technology, Peking University, Beijing 100871, China*
[15]*MTA Atomki, P.O. Box 51, Debrecen H-4001, Hungary*
[16]*Department of Physics, Osaka University, Machikaneyama-machi 1-1, Osaka 560-0043 Toyonaka, Japan*
[17]*Department of Physics, Faculty of Science and Technology, Tokyo University of Science, 2641 Yamazaki, Noda, Chiba, Japan*
[18]*INFN, Sezione di Milano, via Celoria 16, I-20133 Milano, Italy*
[19]*Institut für Kernphysik, Technische Universität Darmstadt, D-64289 Darmstadt, Germany*
[20]*Department of Physics, Sungkyunkwan University, Suwon 440-746, Republic of Korea*
[21]*Istituto Nazionale di Fisica Nucleare, Complesso Universitario di Monte S. Angelo, I-80126 Napoli, Italy*
[22]*Dipartimento di Fisica, Università di Napoli Federico II, Complesso Universitario di Monte S. Angelo, I-80126 Napoli, Italy*
[23]*CEA, DAM, DIF, 91297 Arpajon cedex, France*
[24]*Instituto de Fsica Corpuscular, CSIC-University of Valencia, E-46980 Paterna, Spain*
[25]*Nuclear Engineering Division, Argonne National Laboratory, Argonne, Illinois 60439, USA*
[26]*Department of Nuclear Physics, Research School of Physical Sciences and Engineering, Australian National University, Canberra, Australian Capital Territory 0200, Australia*
[27]*IKP, University of Cologne, D-50937 Cologne, Germany*
[28]*Wright Nuclear Structure Laboratory, Yale University, New Haven, Connecticut 06520-8120, USA*
[29]*Instituut voor Kern- en StralingsFysica, K.U. Leuven, B-3001 Heverlee, Belgium*
[30]*Advanced Science Research Center, Japan Atomic Energy Agency, Tokai, Ibaraki, 319-1195, Japan*
[31]*Department of Physics, University of Surrey, Guildford GU2 7XH, United Kingdom*

(Received 31 January 2014; published 1 April 2014)

A low-lying state in $^{131}In_{82}$, the one-proton hole nucleus with respect to double magic ^{132}Sn, was observed by its γ decay to the $I^{\pi} = 1/2^{-}$ β-emitting isomer. We identify the new state at an excitation energy of $E_x = 1353$ keV, which was populated both in the β decay of $^{131}Cd_{83}$ and after β-delayed neutron emission from $^{132}Cd_{84}$, as the previously unknown $\pi p_{3/2}$ single-hole state with respect to the ^{132}Sn core. Exploiting this crucial new experimental information, shell-model calculations were performed to study the structure of experimentally inaccessible $N = 82$ isotones below ^{132}Sn. The results evidence a surprising absence of proton subshell closures along the chain of $N = 82$ isotones. The consequences of this finding for the evolution of the $N = 82$ shell gap along the r-process path are discussed.

DOI: 10.1103/PhysRevLett.112.132501 PACS numbers: 23.40.-s, 21.10.Pc, 27.60.+j, 21.60.Cs

The shell structure of the atomic nucleus is one of the crucial ingredients in understanding the stability of this mesoscopic system. It has been well understood since the pioneering work of Goeppert-Mayer, and Haxel, Jensen, and Suess, who realized that the experimental evidence for nuclear magic numbers could be explained by assuming a strong spin-orbit interaction, which generates large shell and subshell gaps [1,2]. However, it has been recognized for more than 20 years now that the single-particle ordering which underlies nuclear shell structure changes in regions far off the valley of stability, where nuclei have a large excess of neutrons (or a large N/Z ratio). The understanding of this shell evolution is one of the key topics in current nuclear structure research.

The region around ^{132}Sn, a particle-bound spherical nucleus, is of particular importance in this respect since it is the only region around a heavy, neutron-rich doubly closed shell nucleus far off stability (eight neutrons relative to the last stable isotope ^{124}Sn) for which spectroscopic information can be obtained. ^{132}Sn and its nearest Sn and $_{51}$Sb neighbors have been studied in detail in the past [3–5] and consequently almost all the neutron single-particle and hole states as well as the proton single-particle states with respect to ^{132}Sn are firmly established. Below ^{132}Sn, however, experimental information is scarce: along the $N = 82$ chain of isotones, masses are known only for ^{131}In and ^{130}Cd [6] while β-decay half-lives are measured down to ^{129}Ag [7]. Energies of excited states are available for ^{131}In, ^{130}Cd, and ^{128}Pd [8–10]. While there is consensus about the magic nature of ^{132}Sn, even further from stability, below ^{132}Sn, a weakening of magicity, and in particular a reduction of the $N = 82$ gap, was predicted long ago [11]. Clear experimental evidence for such a "quenching" of the $N = 82$ gap is however still lacking [8–10,12].

Besides the nuclear structure aspect, the lack of experimental information for lighter isotopes along the $N = 82$ line is also regrettable with respect to nuclear astrophysics. These nuclei play a key role in the dynamics (e.g., time scale and neutron density) of the rapid neutron-capture process of nucleosynthesis, the so-called r-process, since they act as a bottleneck for the reaction flow. The unknown evolution of the shell structure in this region is one of the main sources of nuclear physics uncertainty in r-process calculations. Theoretical models have to be relied upon whose predictions for regions far off stability diverge significantly. Since the nuclear physics uncertainties can have as much influence on the r-process abundances as the astrophysical environment, they currently prevent a reliable extraction of site-specific signatures from observational data [13].

To amend this unsatisfactory situation we present in this work the experimental determination of the energy of the $\pi p_{3/2}$ single-hole state in ^{132}Sn. Then, exploiting this new information, we study for the first time the spectroscopic properties of the experimentally inaccessible $N = 82$ isotones on the r-process path below ^{132}Sn using the nuclear shell model (SM). These properties depend on the same sequence of proton single-particle orbitals (SPOs) as that of the $N = 50$ isotones below ^{100}Sn, one major neutron shell below. The relevant proton SPOs being filled between $_{28}$Ni and $_{50}$Sn are $0f_{5/2}$, $1p_{3/2}$, $1p_{1/2}$, and $0g_{9/2}$. In the ^{100}Sn region [14,15], extrapolated gaps of significant size between the $1p_{3/2}$ and $1p_{1/2}$ (1.28 MeV) and the $1p_{1/2}$ and $0g_{9/2}$ (0.65 MeV) SPOs lead to proton subshell closures at $Z = 38$ and 40. As a result the stable $N = 50$ isotones ^{88}Sr and ^{90}Zr show typical signatures of closed-shell nuclei, such as high excitation energies of the first excited 2^+ states, $E(2^+)$, and maxima of the two-proton gap, Δ_{2p} [defined here as $\Delta_{2p} = M(Z+2,N) + M(Z-2,N) - 2M(Z,N)$, where $M(Z,N)$ is the mass of a nucleus with Z protons and N neutrons] as illustrated in Figs. 1(a) and 1(b) (filled black boxes). For this region systematic shell-model calculations have been performed in the past [14–16] which successfully describe the vast amount of available experimental data, including the properties of the $N = 50$ isotones below ^{100}Sn [blue asterisks in Figs. 1(a) and 1(b)].

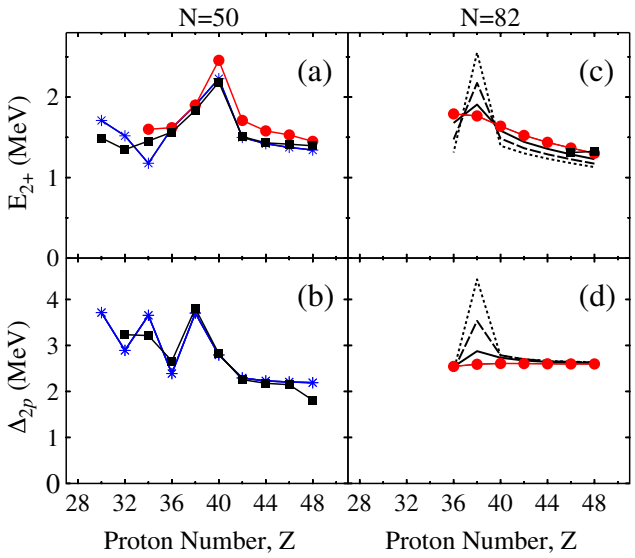

FIG. 1 (color online). (a) Experimental energies of the first excited 2^+ states, $E(2^+)$ and (b) proton gaps, Δ_{2p}, in even $N = 50$ isotones (filled black boxes) compared to the results of the shell-model calculations of Ref. [15] (blue asterisks). The results of new SM calculations (present work), using realistic interactions derived in the same way as the ones used in the calculations for the $N = 82$ isotones, are shown as filled red circles. (c) Energies of the first excited 2^+ states, $E(2^+)$, and (d) proton gaps, Δ_{2p}, for the $N = 82$ isotones as calculated in the present work (filled red circles). The experimental 2^+ energies in ^{130}Cd and ^{128}Pd (filled black boxes) are included for comparison [9,10]. The black lines (solid, dashed, and dotted) represent the results of SM calculations assuming an increase of the $1p$ splitting by 0.5, 1.0, and 1.5 MeV, respectively.

In the ^{132}Sn region, only the position of the proton $1p_{1/2}$ SPO relative to the $0g_{9/2}$ SPO, i.e., the $Z = 40$ gap, is known [4] from the excitation energy of a β-decaying $(1/2^-)$ isomer in ^{131}In ($T_{1/2} = 350(50)$ ms). A more precise value of this energy has been obtained recently from mass measurements [17] indicating a gap of only 365 (8) keV, corresponding to a reduction of nearly 300 keV as compared to the same gap at $N = 50$. The positions of the $1p_{3/2}$ and $0f_{5/2}$ SPOs are unknown. While the deeply bound $0f_{5/2}$ orbital is not expected to play a major role in the description of the $N = 82$ isotones down to $_{40}$Zr and $_{38}$Sr, the position of the $1p_{3/2}$ SPO relative to its spin-orbit partner orbital $1p_{1/2}$ is crucial. This spin-orbit splitting determines whether a proton subshell closure exists in the major $Z = 28$–50 shell at $N = 82$. Its experimental determination is therefore of the utmost importance.

The decay of the second excited state in ^{131}In, populated in the radioactive decay of ^{131}Cd and ^{132}Cd, has been observed in an experiment performed at the Radioactive Isotope Beam Factory at RIKEN in the framework of the EURICA project [18,19]. A ^{238}U beam with a kinetic energy of 345 MeV/u and an average intensity of 8–10 pnA was directed onto a Be target placed in front of the BigRIPS separator [20]. The neutron-rich Cd isotopes were produced by projectile fission, identified event by event by the BigRIPS separator and finally implanted into the WAS3ABi array, a stack of highly segmented silicon strip detectors. The γ-rays emitted after the decay of the radioactive nuclei were detected by the EURICA array. EURICA comprises 84 germanium detectors arranged in a close geometry around the Si detectors assuring a high γ-ray detection efficiency. Figure 2 shows the γ-ray spectra observed in prompt coincidence with the first decay event detected within one mm in each of the three dimensions from the implantation position of a ^{131}Cd (respectively, ^{132}Cd) ion in WAS3ABi. The time window between the implantation and the decay was limited to 210 ms for ^{131}Cd and 300 ms for ^{132}Cd, corresponding to roughly three times their respective half-lives [$T_{1/2} = 68(3)$ ms for ^{131}Cd and $T_{1/2} = 97(10)$ ms for ^{132}Cd [21]]. The decay γ-ray spectrum of ^{132}Cd contains only one line at an energy of 988 keV. The same line is also visible in the decay spectrum of ^{131}Cd, in which several additional high-energy transitions in the ranges 3–4 and 5–6 MeV are observed [22]. In ^{131}In, the lowest core-excited three-quasiparticle states are known to have excitation energies larger than 3.5 MeV [8]. Below this energy at most two additional states are expected besides the known $(9/2^+)$ ground state and the β-decaying $(1/2^-)$ isomer, namely the $3/2^-$ and $5/2^-$ proton single-hole states. We therefore assign the 988 keV γ-ray as decaying from the second excited state in ^{131}In at an excitation energy of 1353 keV, with a spin of either $3/2^-$ or $5/2^-$, to the first excited $(1/2^-)$ level at 365(8) keV. A decay branch to the $(9/2^+)$ ground state is unlikely, due to angular momentum selection rules.

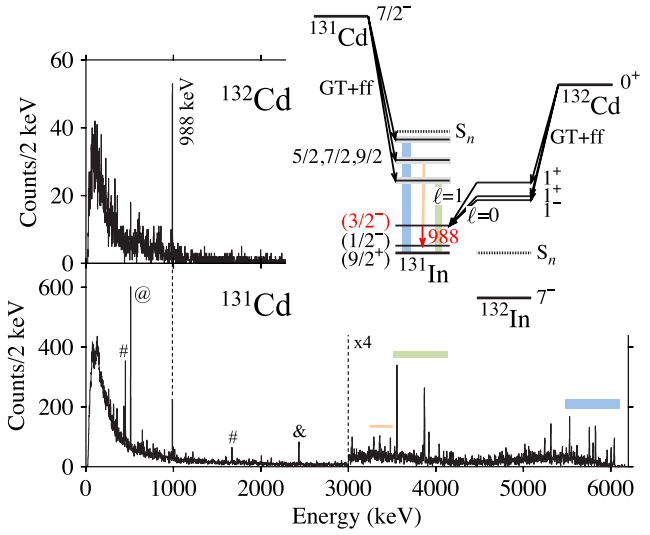

FIG. 2 (color online). Spectra of γ-rays detected in prompt coincidence with the β decay of ^{132}Cd (upper panel) and ^{131}Cd (lower panel). The lines labeled with symbols correspond to known transitions in ^{130}In (#), populated after β-delayed neutron emission from ^{131}Cd, in ^{131}Sn (&), populated in the β decay of the daughter nucleus ^{131}In, and the annihilation of positrons from the pair creation of high-energy γ-rays in the Ge detectors (@). The inset shows a schematic decay scheme for ^{131,132}Cd.

Unfortunately it is not possible to unequivocally assign a spin value to the newly established state solely on the basis of the available experimental information. However, there is a strong argument from systematics favoring a $3/2^-$ ($1p_{3/2}$ SPO) over a $5/2^-$ ($0f_{5/2}$ SPO) assignment. In Fig. 3 the splitting of several $1p$, $1d$, and $1f$ spin-orbit partner orbitals in the vicinity of the neutron-rich double magic nuclei ^{78}Ni, ^{132}Sn, and ^{208}Pb is compared to the energy of the neighboring $0f_{5/2}$, $0g_{7/2}$, and $0h_{9/2}$ orbitals, respectively. All energies are quoted relative to the lowest spin-orbit partner. While, as expected, the spin-orbit splitting slightly increases with angular momentum (see for example the proton $1p$, $1d$, and $1f$ pairs in ^{78}Ni, ^{132}Sn, and ^{208}Pb, respectively), the $0f_{5/2}$, $0g_{7/2}$, or $0h_{9/2}$ orbital does not interlope the spin-orbit pair in any of the cases. It actually does not even come closer than about 900 keV. Duflo and Zuker [23] parametrized the nuclear monopole Hamiltonian and adjusted it to 90 experimental energies of particle and hole states outside double magic cores all over the chart of nuclides, from ^{16}O to ^{208}Pb. The results of this global fit, including the prediction of the relative positions of the $1p_{3/2}$ and $0f_{5/2}$ proton-hole states in ^{132}Sn with respect to the $1p_{1/2}$ SPO (1.1 and 3.7 MeV, respectively), are shown as dashed lines in Fig. 3. Based on this prediction, the experimental energy systematics, and similarities between the experimental decay schemes of ^{131}Cd and ^{207}Hg [22], we tentatively assign spin $3/2^-$ to the newly established state in ^{131}In at an excitation energy of 1353 keV. With respect to the unknown position of the

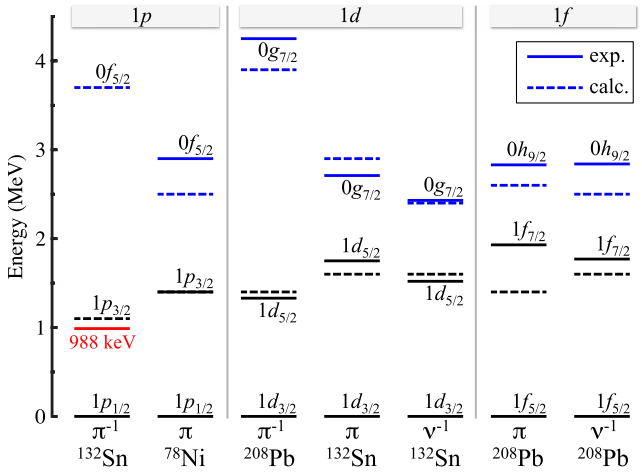

FIG. 3 (color online). Energy systematics of several $1p$, $1d$, and $1f$ spin-orbit partner orbitals in the vicinity of the neutron-rich double magic nuclei ^{78}Ni, ^{132}Sn, and ^{208}Pb compared to the position of the neighboring $0f_{5/2}$, $0g_{7/2}$, and $0h_{9/2}$ SPOs (see text for details). Experimental (calculated) values from Ref. [23] are shown as solid (dashed) lines. For ^{78}Ni, shell-model extrapolated energies are replacing the unknown experimental ones. (Note that for $1p_{3/2}$ both lines coincide.)

fourth proton single-hole state, namely $0f_{5/2}$, we infer from Fig. 3 that it is unlikely to be located at an energy below 2.2 MeV with respect to the $1p_{1/2}$ SPO.

Employing this crucial new piece of experimental information, shell-model calculations were performed to study the properties of the $N = 82$ isotones down to ^{122}Zr and ^{120}Sr. These calculations employ a two-body effective interaction derived from the CD-Bonn nucleon-nucleon potential renormalized by way of the $V_{\text{low-k}}$ approach [24]. Specifically, the interaction is constructed by assuming ^{132}Sn as closed core and considering the full $N = 50$–82 major shell for neutrons (i.e., the $0g_{7/2}$, $1d_{5/2}$, $1d_{3/2}$, $2s_{1/2}$, and $0h_{11/2}$ orbitals) and the $Z = 28$–50 shell for protons (i.e., the $0f_{5/2}$, $1p_{3/2}$, $1p_{1/2}$, and $0g_{9/2}$ orbits). The single-particle energies were taken from experiment (from Ref. [5] and the present work) except for the still unknown $0f_{5/2}$ SPO for which a value of 2.6 MeV relative to $0g_{9/2}$ was assumed. To check the quality of the interaction first the results were inspected for all Pd, Cd, In, and Sn isotopes with $N \leq 82$, for which experimental information on excited states is available. This comparison revealed two deficiencies of the interaction which subsequently have been corrected: the pairing in the proton-proton ($\pi\pi$) channel is too strong, and the multipole part in the neutron-neutron ($\nu\nu$) and $\pi\nu$ channels is too weak. Using the modified set of interactions, the experimental-level schemes and transition rates of $^{126\text{–}130}$Sn [25], ^{130}In [12], ^{127,128}Cd [26,27], ^{130}Cd [9], and ^{126,128}Pd [10] are all nicely reproduced.

Once such a consistent description of the relevant features in the region was obtained, the basic properties of the $N = 82$ isotones were calculated. Figures 1(c) and 1(d) show the resulting excitation energies of the first excited 2^+ states, $E(2^+)$, as well as the two-proton gap, Δ_{2p}, as a function of the proton number Z (red filled circles). To account for Coulomb repulsion and to be consistent with the $N = 50$ results, a general shift of $+300$ keV was added to all diagonal $\pi\pi$ two-body matrix elements in the calculation of Δ_{2p}. In contrast to the behavior of the same quantities for the $N = 50$ isotones [compare Figs. 1(a) and 1(b)], here $E(2^+)$ increases only smoothly from $_{48}$Cd down to $_{36}$Kr, while the two-proton gap Δ_{2p} remains constant within 70 keV in the same Z range. Note that this behavior of $E(2^+)$ and Δ_{2p} does not depend on the general $\pi\pi$ pairing reduction to 88%, which was applied in order to better describe the excited-state energies in ^{130}Cd and ^{128}Pd. Figures 1(c) and 1(d) clearly show that the diminishment of the $0g_{9/2}$–$1p_{1/2}$ and $1p_{1/2}$–$1p_{3/2}$ gaps by about 300 keV each when moving one major neutron shell up from $N = 50$ towards $N = 82$ is sufficient to completely erode the proton subshell structure in the chain of $N = 82$ isotones. To challenge the predictive power of our approach, the 2^+ excitation energies of the $N = 50$ isotones have been calculated within the shell-model framework in the same way as described above for the $N = 82$ isotones, i.e., using a realistic effective interaction derived from the CD-Bonn potential. A good agreement between calculated (filled red circles) and experimental (filled black boxes) energies was found as shown in Fig. 1(a).

At this point we would like to stress that the disappearance of the proton subshell structure neither depends on the tentative assignment of spin $3/2^-$ to the newly identified state at 1353 keV nor on the position of the $0f_{5/2}$ proton-hole state. To prove this claim additional SM calculations were performed, first by exchanging the positions of the $1p_{3/2}$ and $0f_{5/2}$ SPOs and second by increasing the unknown energy of the $0f_{5/2}$ state from 2.6 to 4.5 MeV. In the relevant range of Z, the behavior of $E(2^+)$ and Δ_{2p} is not affected by these drastic modifications. It is really the mere proximity (less than 1 MeV) of the next SPO to the $1p_{1/2}$ orbit, independent of its character, that is solely responsible for the disappearance of the proton subshell closure. A hypothetical increase of the energy gap between the $1p_{1/2}$ and the next SPO in the SM calculations immediately leads to the development of maxima at $Z = 38$ for both $E(2^+)$ and Δ_{2p} and thus a restoration of the proton subshell closure at $Z = 38$ [compare the black lines in Figs. 1(c) and 1(d)]. The disappearance of the $Z = 38$, 40 subshell closures is the first evidence for a changing shell structure in the region of neutron-rich nuclei below ^{132}Sn.

As we will discuss now, this finding has an important impact on the evolution of the $N = 82$ neutron-shell gap in the region most relevant for the r process. It is well known that a given magic shell gap attains a maximum value when the number of nucleons of the other kind is magic, too. This

effect is referred to as mutual support of magicities [28]. Moving away from a double magic nucleus along a semimagic chain of isotones (or isotopes), the neutron (proton) gap then decreases rapidly due to enhanced cross-shell excitations. An inspection of the compilation of experimental masses [6] reveals that this behavior is observed without any exception all over the chart of nuclides (for an overview see Fig. 8 of Ref. [29]). In the absence of a subshell structure the gap size reaches a minimum in the middle of the major shell. However, in regions of proton (or neutron) subshell closures the cross-shell excitations are hampered and local maxima are observed for the size of the neutron (proton) gap. A prominent example of such behavior is the $N = 50$ gap around the $Z = 38$, 40 subshell closures discussed above. These subshell closures are at the origin of the stability of the $N = 50$ gap from $Z = 48$ down to $Z = 38$. It is only below the $Z = 38$ subshell closure that this gap shrinks significantly towards $Z = 32$ [30,31]. For the $N = 82$ neutron gap, in contrast, due to the disappearance of the proton subshell structure, a significant reduction is expected already between Sn and Zr, similar to the one observed above ^{132}Sn between Sn and $_{60}$Nd ($\approx$2.5 MeV).

Finally, we confront this expectation of a reduction of the $N = 82$ gap between Sn and Zr with the predictions of two of the theoretical mass models most frequently employed in r-process calculations today, namely, the microscopic-macroscopic finite-range droplet model (FRDM) [32] and a model based on the self-consistent Hartree-Fock-Bogoliubov theory (HFB-24) [29]. Although based on very different physics ingredients, both models reproduce the more than 2300 experimentally known masses, to which they are fitted, with an average deviation below 600 keV. However, severe differences are observed when predictions of unknown masses are compared. While the $N = 82$ gap is predicted to remain nearly constant from $Z = 50$ down to $Z = 40$ by the FRDM model, a significant quenching is prognosticated by the HFB-24 approach. In light of the new findings presented here, we suggest that in future r-process calculations preference should be given to the HFB-24 model, which predicts a $N = 82$ evolution consistent with the expectations based on the changes of shell structure in this region.

To conclude, we presented the measurement of the energy of the $1p_{3/2}$ proton-hole state in ^{132}Sn. This energy constitutes a crucial piece of information, allowing for the study of the structure of experimentally inaccessible $N = 82$ isotones on the r-process path below ^{132}Sn using the nuclear shell model and a modern realistic interaction. Our study provides robust evidence for the disappearance of the $Z = 38$, 40 proton subshell closures at $N = 82$ and thereby manifests for the first time changes in the shell structure in this region far off stability. As a consequence of these changes a significant reduction of the $N = 82$ gap in the region of the r-process path is expected. We believe that for the time being, until the lighter $N = 82$ isotones eventually become accessible for direct mass measurements, this indirect evidence for a quenching of the $N = 82$ neutron-shell gap in the region of interest provides a valuable guidance for the choice of mass models to be employed in r-process calculations.

We thank the staff of the RIKEN Nishina Center accelerator complex for providing stable beams with high intensities to the experiment. We acknowledge the EUROBALL Owners Committee for the loan of germanium detectors and the PreSpec Collaboration for the readout electronics of the cluster detectors. This work was supported by the Spanish Ministerio de Ciencia e Innovación under Contracts No. FPA2009-13377-C02 and No. FPA2011-29854-C04, the Generalitat Valenciana (Spain) under grant PROMETEO/2010/101, the Japanese government under contract KAKENHI (25247045), the National Research Foundation of Korea (NRF) grant funded by the Korea government (MEST) (No. NRF-2012R1A1A1041763), the Priority Centers Research Program in Korea (2009-0093817), OTKA contract number K-100835, the European Commission through the Marie Curie Actions call FP7-PEOPLE-2011-IEF under Contract No. 300096, the U.S. Department of Energy, Office of Nuclear Physics, under Contract No. DE-AC02-06CH11357 and the German BMBF (No. 05P12RDCIA and 05P12RDNUP) and HIC for FAIR.

*Corresponding author.
andrea.jungclaus@csic.es
†Present address: Department of Physics, Universty of Notre Dame, Notre Dame, Indiana 46556, USA.

[1] M. Goeppert-Mayer, Phys. Rev. **74**, 235 (1948); **75**, 1969 (1949); **78**, 16 (1950).
[2] O. Haxel, J. H. D. Jensen, and H. E. Suess, Phys. Rev. **75**, 1766 (1949).
[3] K. L. Jones *et al.*, Nature (London) **465**, 454 (2010).
[4] B. Fogelberg *et al.*, Phys. Rev. C **70**, 034312 (2004).
[5] H. Grawe, K. Langanke, and G. Martínez-Pinedo, Rep. Prog. Phys. **70**, 1525 (2007).
[6] M. Wang, G. Audi, A. H. Wapstra, F. G. Kondev, M. MacCormick, X. Xu, and B. Pfeiffer, Chin. Phys. C **36**, 1603 (2012).
[7] K.-L. Kratz, B. Pfeiffer, F.-K. Thielemann, and W. B. Walters, Hyperfine Interact. **129**, 185 (2000).
[8] M. Górska *et al.*, Phys. Lett. B **672**, 313 (2009).
[9] A. Jungclaus *et al.*, Phys. Rev. Lett. **99**, 132501 (2007).
[10] H. Watanabe *et al.*, Phys. Rev. Lett. **111**, 152501 (2013).
[11] J. Dobaczewski, I. Hamamoto, W. Nazarewicz, and J. A. Sheikh, Phys. Rev. Lett. **72**, 981 (1994).
[12] I. Dillmann *et al.*, Phys. Rev. Lett. **91**, 162503 (2003).
[13] A. Arcones and G. Martínez-Pinedo, Phys. Rev. C **83**, 045809 (2011).
[14] T. Faestermann, M. Górska, and H. Grawe, Prog. Part. Nucl. Phys. **69**, 85 (2013).

[15] A. F. Lisetskiy, B. A. Brown, M. Horoi, and H. Grawe, Phys. Rev. C **70**, 044314 (2004).
[16] C. B. Hinke *et al.*, Nature (London) **486**, 341 (2012).
[17] A. Kankainen *et al.*, Phys. Rev. C **87**, 024307 (2013).
[18] S. Nishimura, Prog. Theor. Exp. Phys. **2012**, 03C006 (2012).
[19] P.-A. Söderström *et al.*, Nucl. Instrum. Methods Phys. Res., Sect. B **317**, 649 (2013).
[20] T. Kubo *et al.*, Prog. Theor. Exp. Phys. **2012**, 03C003 (2012).
[21] M. Hannawald *et al.*, Phys. Rev. C **62**, 054301 (2000).
[22] J. Taprogge *et al.* (to be published).
[23] J. Duflo and A. P. Zuker, Phys. Rev. C **59**, R2347 (1999).
[24] L. Coraggio, A. Covello, A. Gargano, N. Itaco, and T. T. S. Kuo, Prog. Part. Nucl. Phys. **62**, 135 (2009).
[25] ENSDF database, http://www.nndc.bnl.gov/ensdf/.
[26] F. Naqvi *et al.*, Phys. Rev. C **82**, 034323 (2010).
[27] L. Cáceres *et al.*, Phys. Rev. C **79**, 011301(R) (2009).
[28] N. Zeldes, T. S. Dumitrescu, and H. S. Köhler, Nucl. Phys. **A399**, 11 (1983).
[29] S. Goriely, N. Chamel, and J. M. Pearson, Phys. Rev. C **88**, 024308 (2013).
[30] J. Hakala *et al.*, Phys. Rev. Lett. **109**, 032501 (2012).
[31] J. Van Schelt *et al.*, Phys. Rev. Lett. **111**, 061102 (2013).
[32] P. Möller, W. D. Myers, H. Sagawa, and S. Yoshida, At. Data Nucl. Data Tables **59**, 185 (1995); Phys. Rev. Lett. **108**, 052501 (2012).